

Supplemental Information

**Enhanced mucosal SARS-CoV-2 immunity after
heterologous intramuscular mRNA prime/intranasal
protein boost vaccination with a combination adjuvant**

Gabriel Laghlali, Matthew J. Wiest, Dilara Karadag, Prajakta Warang, Jessica J. O'Konek, Lauren A. Chang, Seok-Chan Park, Vivian Yan, Mohammad Farazuddin, Katarzyna W. Janczak, Adolfo García-Sastre, James R. Baker Jr., Pamela T. Wong, and Michael Schotsaert

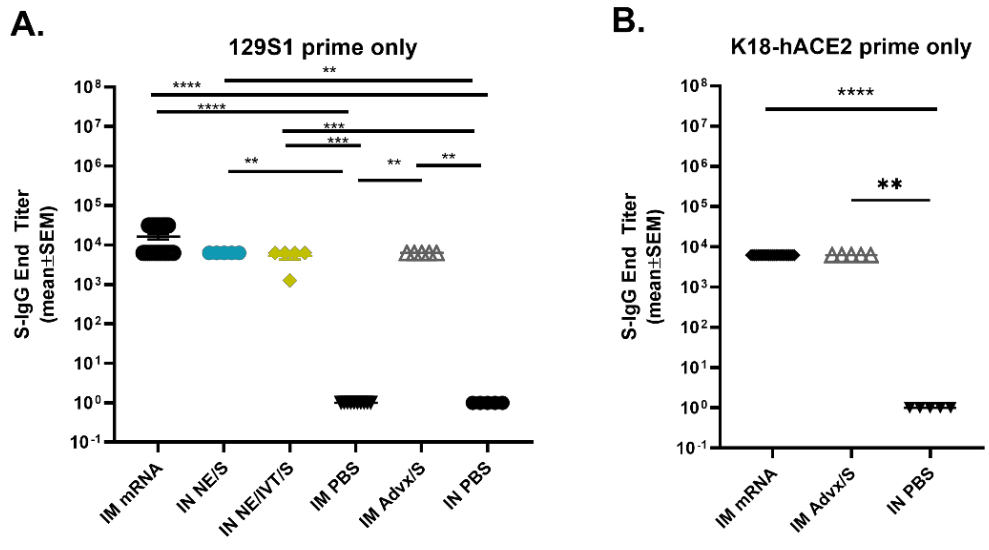


Figure S1: S-specific IgG induced 2 wks post-prime immunization in (A) 129S1 and (B) K18hACE2 mice immunized IM with 0.4 μ g of BNT162b2 mRNA or Advx with 15 μ g S, or IN with 15 μ g S with either NE or NE/IVT or PBS (n=5/grp; * p <0.05, ** p <0.01, *** p <0.001, **** p <0.0001 by Mann-Whitney U test).

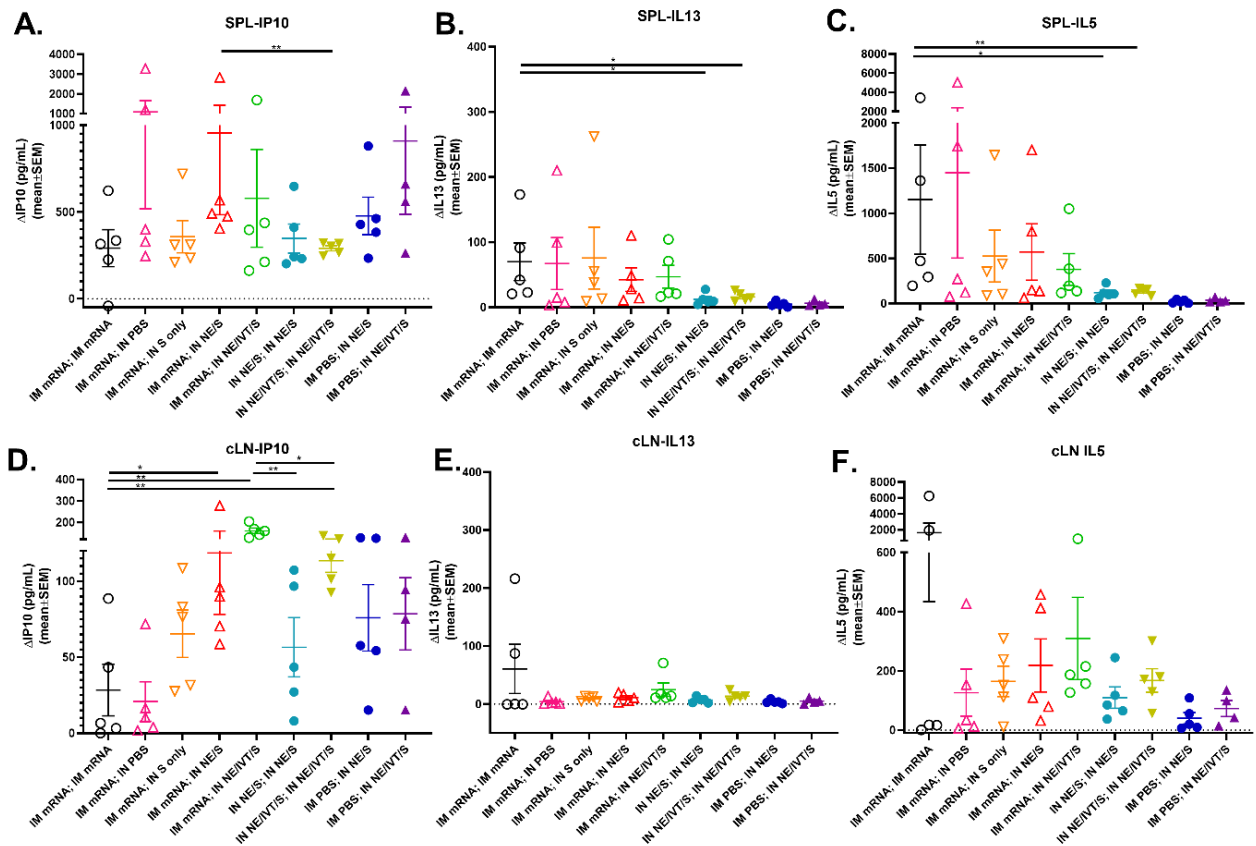
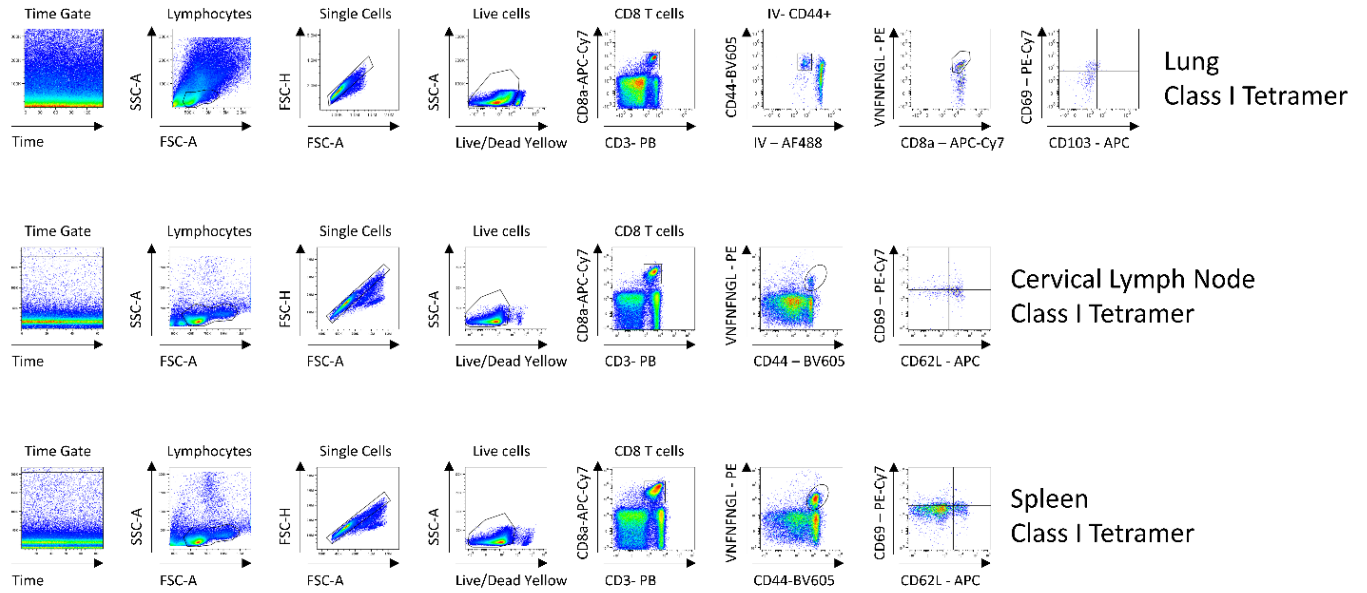


Figure S2: Antigen recall responses assessed in splenocytes and cervical lymph node of twice IN administered mice have suppressed Th2 responses. Splenocytes (A-C) and cLN cellular isolates (D-F) were prepared from mice given prime/boost immunizations with the indicated adjuvant/antigen regimens two weeks after the final immunization. Cells were stimulated *ex vivo* with 25 $\mu\text{g}/\text{mL}$ S protein for 72h, and levels of secreted (A, D) IP-10 (B, E) IL-13, and (C, F) IL-5 were measured by multiplex immunoassay. Values were assessed relative to unstimulated cells. (n=4-5/grp; * $p < 0.05$, ** $p < 0.01$ by Mann-Whitney U test shown only for select groups-(full statistical analysis is shown in **Table S1**)).

Class I Tetramer Gating Pathway



Class II Tetramer Gating Pathway

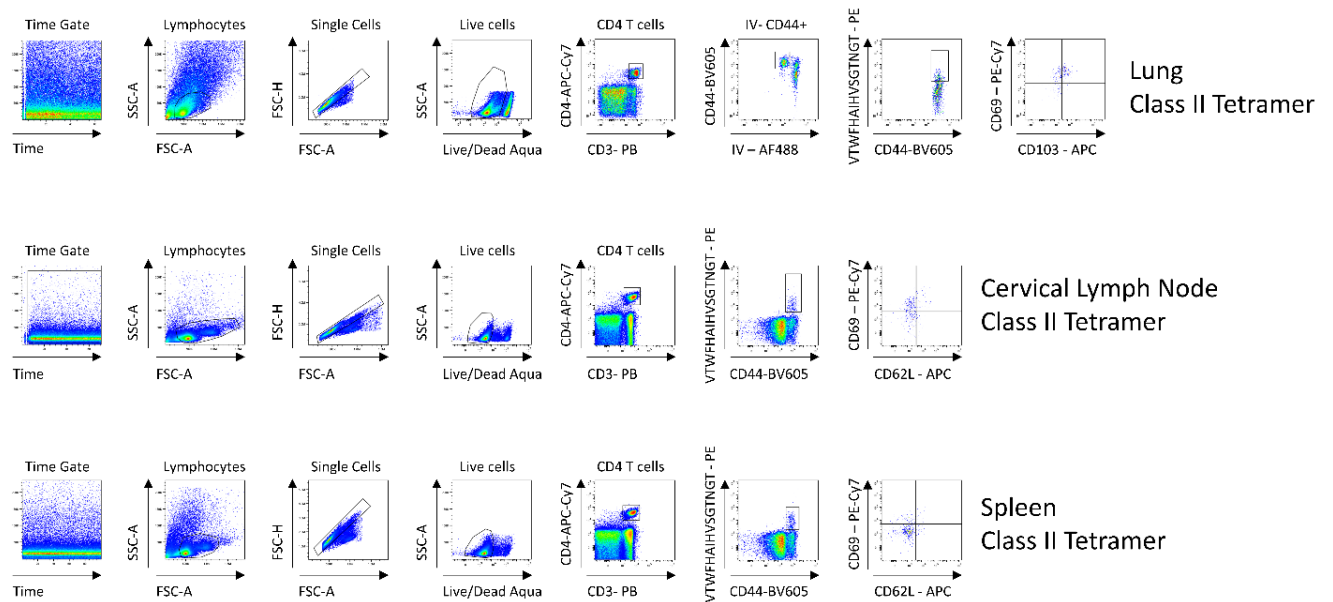
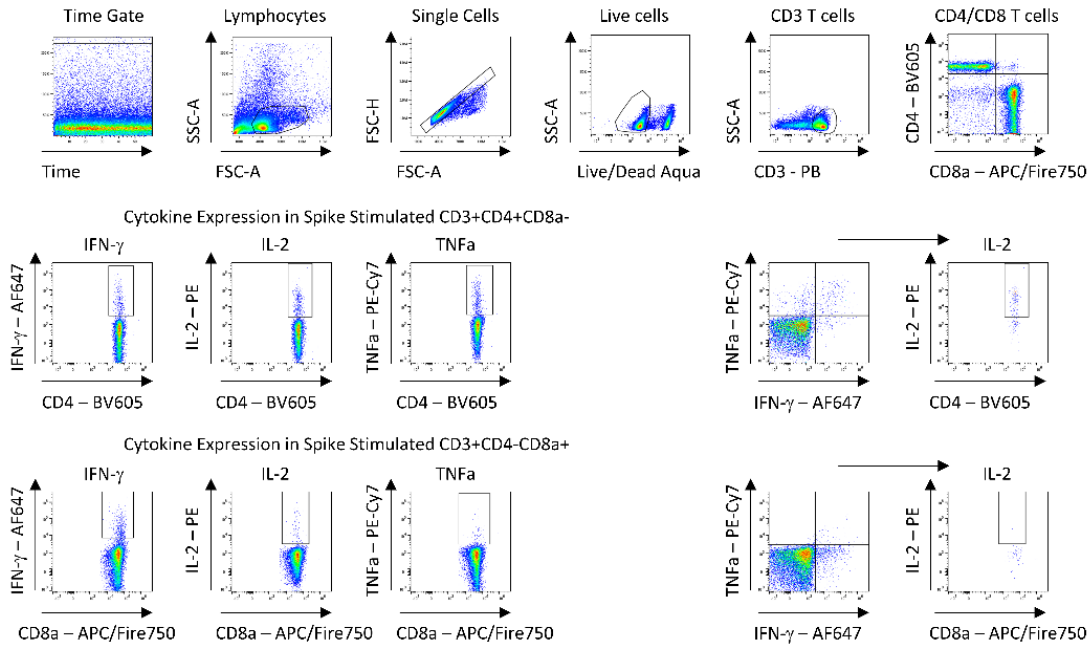


Figure S3: Gating strategy for Class I and Class II Tetramer staining. Representative gating strategy for tissue resident memory CD8⁺ and CD4⁺ T cells in lung were distinguished by IV⁻CD44⁺Tetramer⁺CD69⁺CD103⁺ expression. Frequency of CD44⁺Tetramer⁺CD69⁺CD62L⁻ expressing CD8⁺ and CD4⁺ T cells were also assessed in the cLN and spleen.

Spleen/cLN ICS Gating Pathway



Lung ICS Gating Pathway

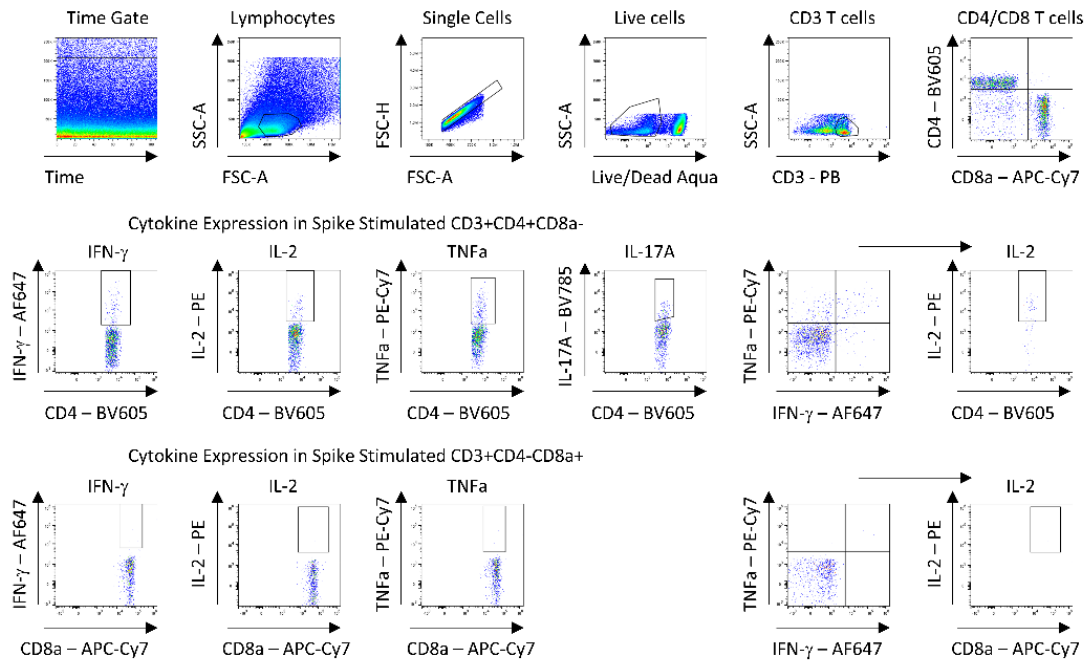


Figure S4: Gating strategy for ICS. Representative gating strategy for cytokine (IFN- γ , IL-2, TNF α , IL-17A) expression in CD4⁺ T and CD8⁺ T cells was evaluated in the spleen and cLN, and lung after 24 hours of stimulation with 25 μ g/mL spike protein in the presence of Brefeldin A for the last 6 hours.

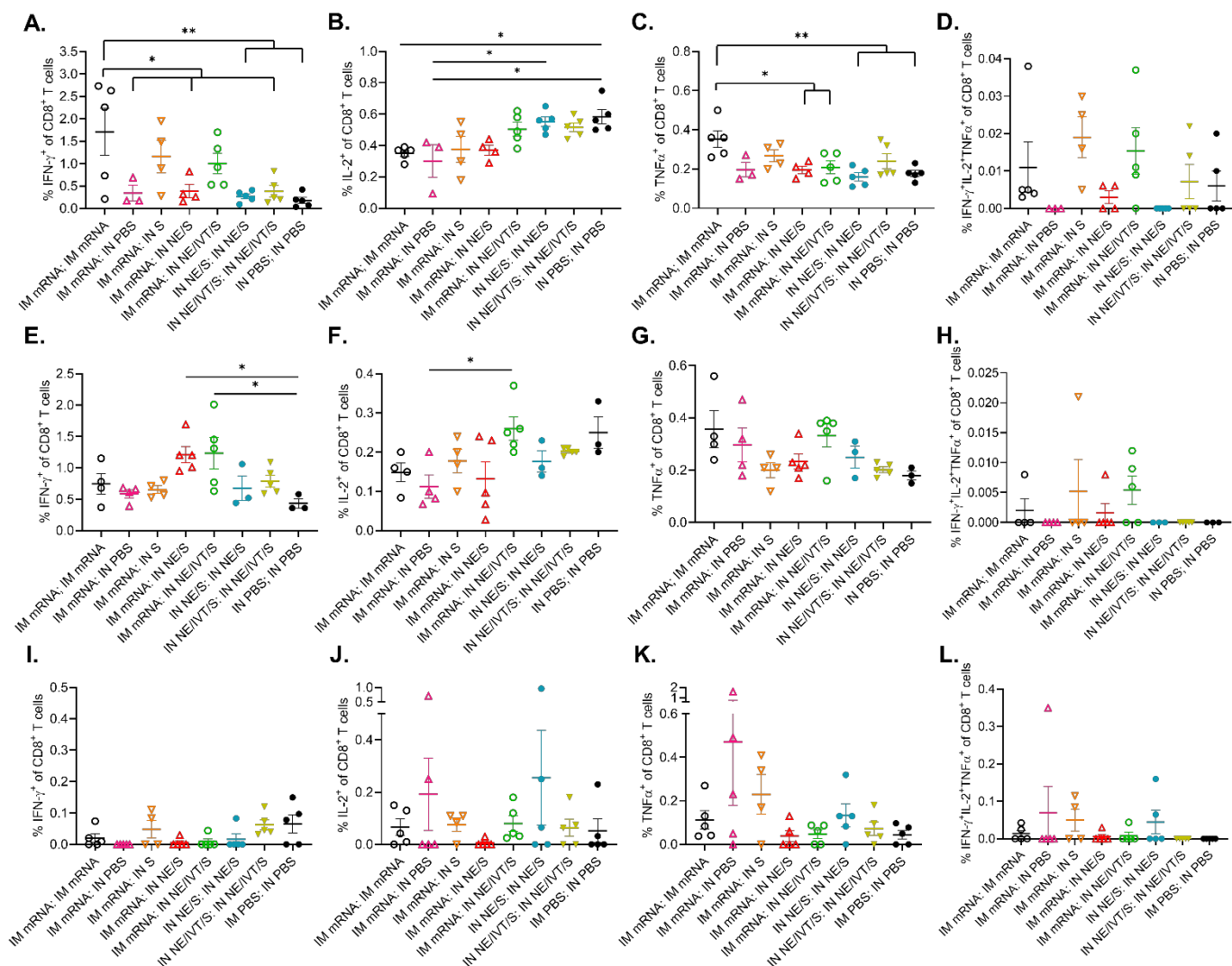


Figure S5: Cytokine expression in CD8⁺ T cells isolated from spleen, cLN, and lung. Frequency of IFN-γ, IL-2, TNFα, and IFN-γ IL-2 TNFα expressing CD8 T cells in cell suspensions isolated from the spleen (A-D), cervical lymph nodes (E-H), and lungs (I-L) of vaccinated mice after 24 hours of stimulation with 25μg/mL spike protein. (n=3-5/grp; **p*<0.05, ***p*<0.01, by One way ANOVA with Tukey post-hoc).

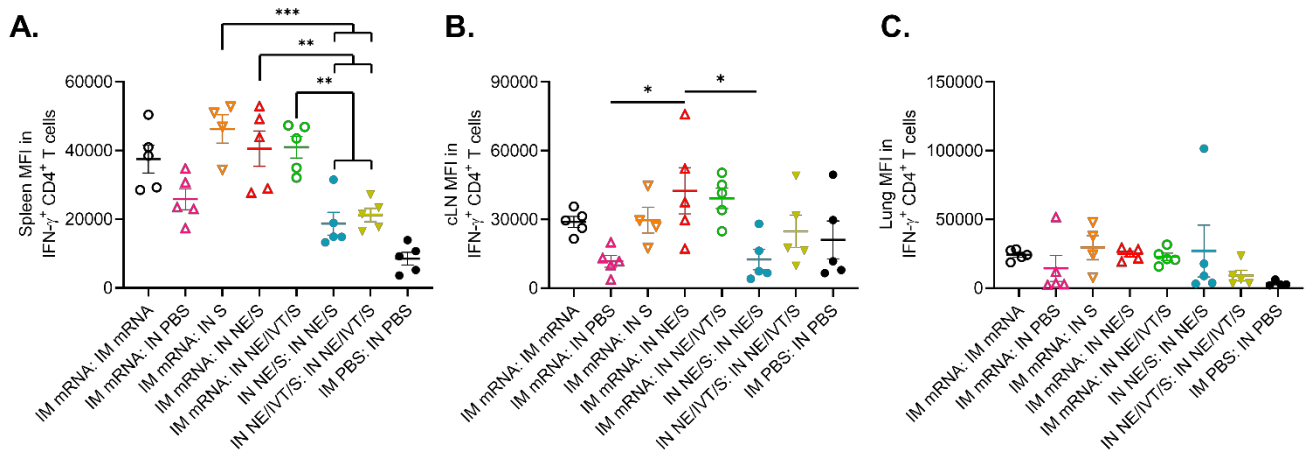


Figure S6: MFI of IFN- γ expressing CD4⁺ T cells. Mean fluorescent intensity of IFN- γ expression in CD4⁺ T cells in spleen (A), cLN (B) and lung (C) cells stimulated with 25 μ g/mL spike protein for 24 hours. (n=4-5/grp; * $p < 0.05$, ** $p < 0.01$, *** $p < 0.001$ by One way ANOVA with Tukey post-hoc test shown for select groups (full statistical analysis is shown in **Table S1**)).

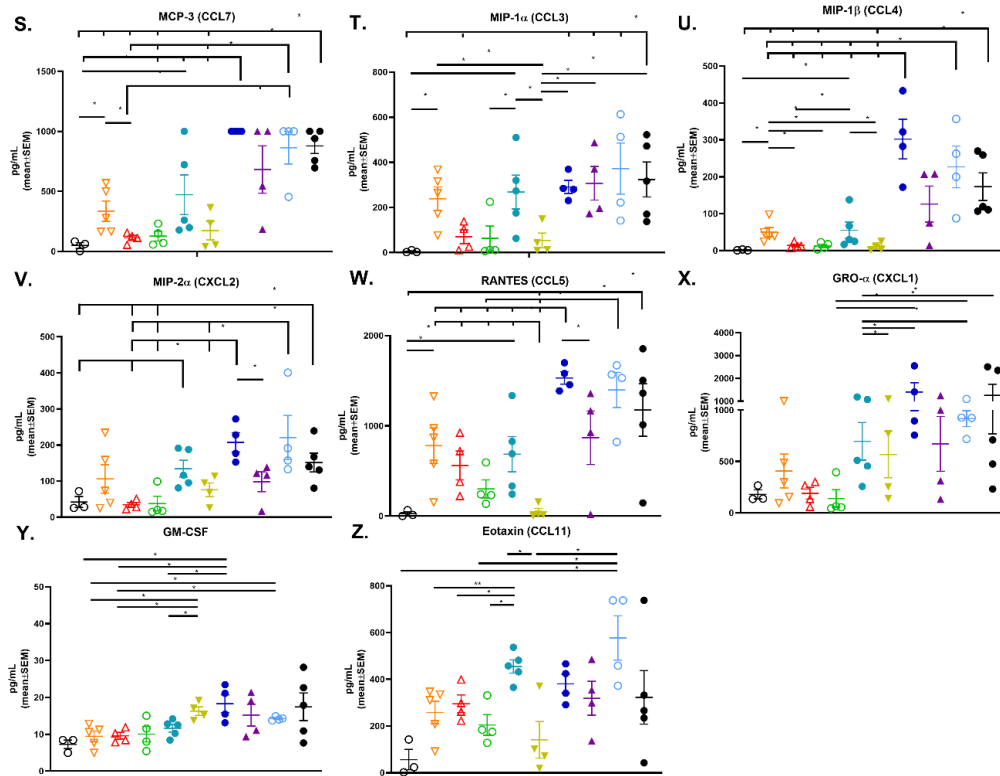


Figure S8: Cytokine production in lung homogenates from 129S1 immunized mice post-challenge demonstrate different host response skewing depending on vaccination type and route. Individual cytokine levels in lung homogenate (shown as heatmap in Figure 7) measured by multiplex immunoassay from immunized 129S1 mice in Figure 7 measured at 4 d.p.i. with 10^4 pfu B.1.351. (A) IFN- γ , (B) IL-2, (C) TNF- α , (D) IL-12p70, (E) IP-10, (F) IL-4, (G) IL-5, (H) IL-13, (I) IL-6, (J) IL-17A, (K) IL-10, (L) IL-22, (M) IL-23, (N) IL-27, (O) IL-18, (P) IL-9, (Q) IL-1 β , (R) MCP-1, (S) MCP-3, (T) MIP-1 α , (U) MIP-1 β , (V) MIP-2 α , (W) RANTES, (X) GRO α , (Y) GM-CSF, (Z) eotaxin ($n=4-5$ /grp; * $p<0.05$, ** $p<0.01$ by Mann-Whitney U test).

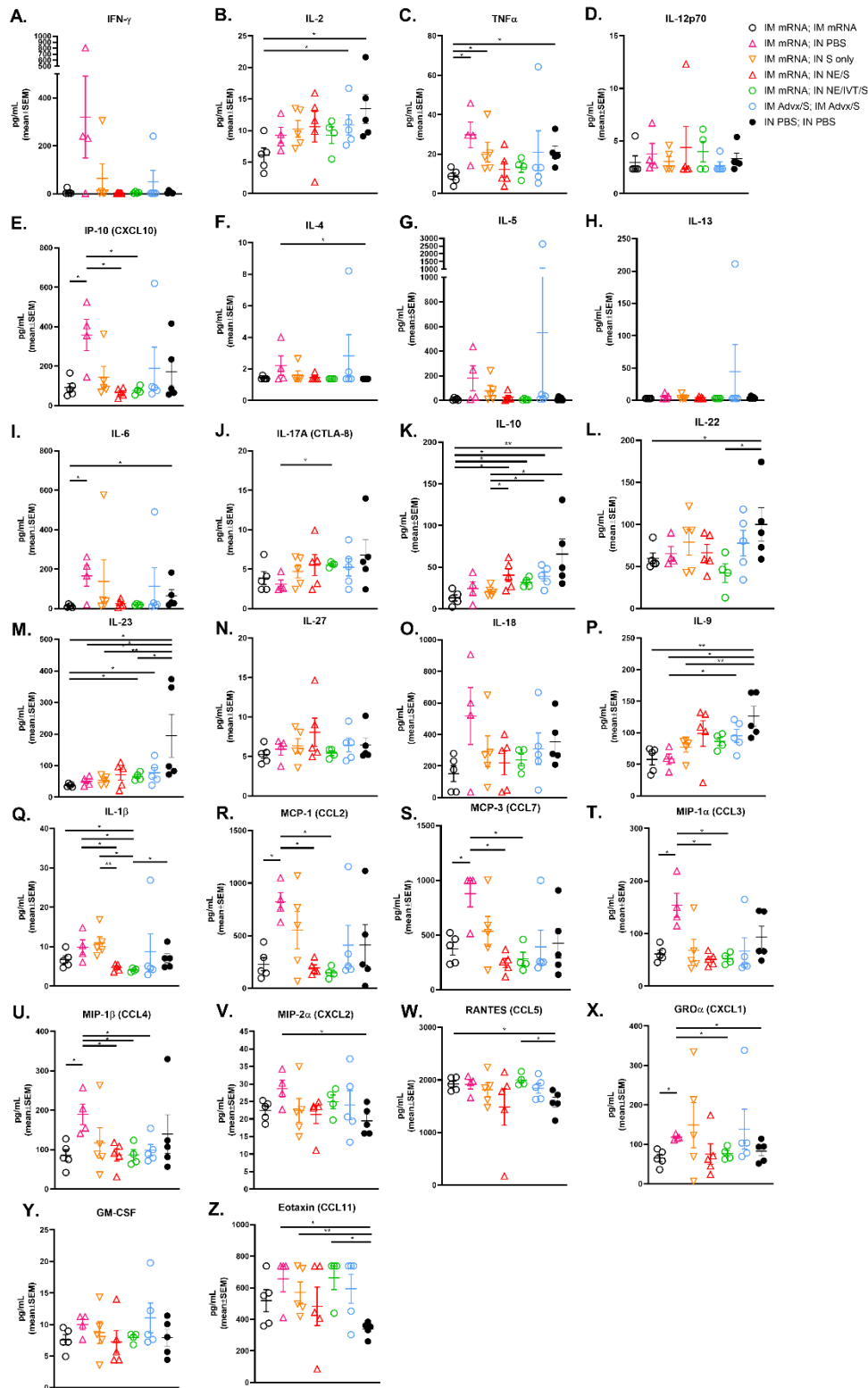


Figure S9: Cytokine production in lung homogenates from K18-hACE2 immunized mice post-challenge demonstrate different host response skewing depending on vaccination type and route. Individual cytokine levels in lung homogenate (shown as heatmap in Figure 7)

measured by multiplex immunoassay from immunized K18-hACE2 mice in Figure 7 measured at 4 d.p.i. with 10^4 pfu BA.5. (A) IFN- γ , (B) IL-2, (C) TNF- α , (D) IL-12p70, (E) IP-10, (F) IL-4, (G) IL-5, (H) IL-13, (I) IL-6, (J) IL-17A, (K) IL-10, (L) IL-22, (M) IL-23, (N) IL-27, (O) IL-18, (P) IL-9, (Q) IL-1 β , (R) MCP-1, (S) MCP-3, (T) MIP-1 α , (U) MIP-1 β , (V) MIP-2 α , (W) RANTES, (X) GRO α , (Y) GM-CSF, (Z) eotaxin ($n=4-5$ /grp; * $p<0.05$, ** $p<0.01$ by Mann-Whitney U test).

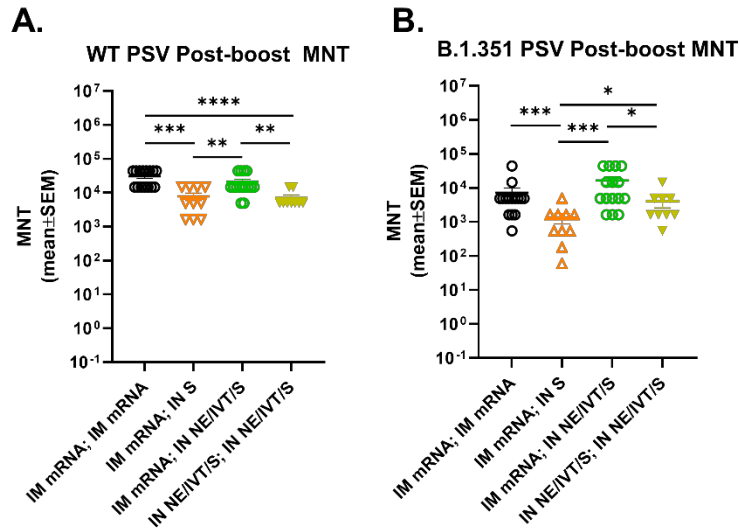


Figure S10: Serum viral neutralizing antibody titers in immunized 129S1 donor mice used for passive serum transfer. 129S1 mice were immunized with IM mRNA prime/boost, IN NE/IVT/S prime/boost or with IM mRNA prime followed by IN boost with S alone or adjuvanted with NE/IVT at a 4 wk interval. Vaccine doses consisted of 0.4 μ g of mRNA and 15 μ g S protein. Neutralizing antibody titers were measured against (A) WT and (B) B.1.351 pseudoviruses. 2wks post-boost, sera were pooled from each treatment group for use in passive transfer experiments ($n=9-15$ /grp; * $p<0.05$, ** $p<0.01$, *** $p<0.001$, **** $p<0.0001$ by Mann-Whitney U test).

TABLE S1: Complete statistical data analysis in figures ($*p < 0.05$, $**p < 0.01$, $***p < 0.001$, $****p < 0.0001$ by Mann-Whitney U test or one way ANOVA with Tukey post-hoc test).

Table S2. Antibodies utilized in flow cytometry.

Antibody	Clone	Source	Catalog
Pacific Blue Anti-Mouse CD3	17A2	Biologend	100214
BV605 Anti-Mouse CD4	RM4-5	Biologend	100548
APC-Cy7 Anti-Mouse CD4	RM4-5	Biologend	100526
APC-Cy7 Anti-Mouse CD8a	53-6.7	Biologend	100714
APC-Fire750 Anti-Mouse CD8a	53-6.7	Biologend	100766
BV605 Anti-Mouse CD44	IM7	Biologend	103047
APC Anti-Mouse CD62L	MEL-14	Biologend	104412
PE-Cy7 Anti-Mouse CD69	H1.2F3	eBioscience	25-0691-82
APC Anti-Mouse CD103	2E7	Biologend	121414
AF647 Anti-Mouse IFN- γ	XMG1.2	Biologend	505814
PE Anti-Mouse IL-2	JES6-5H4	Biologend	503808
PE-Cy7 Anti-Mouse TNF α	MP6-XT22	Biologend	506324
BV785 Anti-Mouse IL-17A	TC11-18H10.1	Biologend	506928
PE-VNFnFNGL	N/A	NIH Tetramer Core	
PE-VTWFHAIHVSGTNGT	N/A	NIH Tetramer Core	